ISSN-1996-918X

Pak. J. Anal. Environ. Chem. Vol. 27, No. 1 (2026) 500716c

http://doi.org/10.21743/pjaec/2026/500716c

Synthesis and Sorption Performance of Pyridyl-Based Imine and its Homocyclic Analogue toward Ni(II) and Cd(II) Ions in Aqueous Solution

Fatima Aziz[1,2], Noureen Khan[1]*, Nelofer Jamil[2], Musarat Riaz[2], Shagufta Fahmid[2]

[1]*Department of Chemistry, Rawalpindi Women University, 6th Road, Satellite Town, Rawalpindi 46300, Pakistan.*

[2]*Department of Chemistry, Sardar Bahadur Khan Women University, Quetta, Pakistan.*

*Corresponding author Email:noureen.khan@rwu.edu.pk

Received 17 October 2025, Revised 14 February 2026, Accepted 15 April 2026

Academic Editor: Najma Memon

Abstract

Nickel and cadmium are toxic heavy metals that pose serious environmental and health concerns due to their persistence and bioaccumulation. It commonly enters aquatic systems through industrial effluents, electroplating, mining, and the disposal of Ni-Cd batteries. Developing efficient sorbents for their removal from water is therefore of great importance. In this study, two imine derivatives were synthesized and evaluated as sorbents for Ni(II) and Cd(II) ions. The first derivative, 3,3′-dimethyl-[1,1′-biphenyl]-4,4′-diyl-bis-(1-(pyridin-2-yl) methanimine) (SB-1), was obtained from aryl diamine and pyridine-2-carboxaldehyde, while the second, 3,3′-dimethyl-[1,1′-biphenyl]-4,4′-diyl-bis-(1-phenylmethanimine) (SB-2), was synthesized using benzaldehyde. Both compounds were characterized by UV–Vis, FT-IR, FAB-MS, and ^{1}H-NMR spectroscopy. Batch adsorption experiments showed that SB-1 achieved maximum adsorption capacities (Qmax) of 16.89 mg/g for Ni(II) and 8.05 mg/g for Cd(II), while SB-2 recorded 12.66 mg/g and 7.42 mg/g, respectively, indicating higher efficiency of SB-1. The Langmuir model best described the adsorption data, suggesting monolayer adsorption on homogeneous surfaces, and R_L values confirmed favorable sorption. Kinetic studies fitted well to the pseudo-second-order model, indicating chemisorption as the main mechanism. Thermodynamic analysis revealed that adsorption by SB-1 was spontaneous, irreversible, and endothermic, whereas SB-2 adsorption was spontaneous, reversible, and exothermic.

Keywords: Imine derivatives, characterization, metal ion adsorption, isotherm studies, kinetic studies, thermodynamic studies.

Introduction

Pyridine, one of the most important nitrogen-containing heterocycles, is widely recognized for its presence in many therapeutic agents and industrial applications [1]. Owing to its versatile reactivity, pyridine can participate in both nucleophilic and electrophilic substitution reactions, undergo N-protonation, and also exhibit unique optical characteristics [2]. Its favorable physical, chemical, and biological properties have led to the development of a wide range of pyridine derivatives with enhanced functionality and reduced toxicity. These derivatives find applications in diverse sectors, including paints, dyes, flavors, perfumes, disinfectants, explosives, and as intermediates in the synthesis of agrochemicals such as herbicides, fungicides, and insecticides [3]. Furthermore, pyridine exhibits a strong binding affinity toward transition metals, enabling the

formation of a wide variety of metal complexes with applications ranging from catalysis to sensing [4]. In particular, amino- or formyl-substituted pyridines readily condense with primary amines to form Schiff bases (imines), which serve as excellent ligands due to the electron-donating and π-accepting properties of the imine nitrogen [5,6]. Pyridine-based Schiff bases, especially ortho-substituted derivatives, provide strong chelation sites through pyridine nitrogen and adjacent unsaturated nitrogen atoms, thereby offering high affinity for metal ions and improved bioactivity [7].

Among hazardous pollutants, cadmium (Cd) and nickel (Ni) are of particular concern due to their low redox potential, persistence, and toxicity. Their release into the environment originates from several anthropogenic activities, including fossil fuel combustion, mining, electroplating, and industrial effluents, as well as the disposal of spent Ni-Cd batteries into landfills, which increases leachate contamination [8,9]. Conventional wastewater treatment processes are often insufficient for the removal of these metals, leading to their discharge into aquatic systems or the use of contaminated water for irrigation. As a result, Ni and Cd can bioaccumulate through the food chain, posing severe risks to plants, aquatic life, and human health. Reported adverse effects include damage to the reproductive, respiratory, urinary, nervous, and cardiovascular systems, as well as potential carcinogenicity [10,11].

Given these concerns, the development of efficient sorbents for Ni(II) and Cd(II) removal is essential. Pyridine-based imines, with their strong binding capability, structural flexibility, and enhanced chelation ability, present a promising class of sorbents. This study focuses on the synthesis and comparative evaluation of a pyridine-based imine and its homocyclic analogue for the adsorptive removal of Ni(II) and Cd(II) ions from aqueous media.

Materials and Methods

Chemicals and reagents

The 3,3′-dimethyl-[1,1′-biphenyl]-4,4′-diamine, benzaldehyde, acetic acid, pyridine-2-carboxaldehyde, solvents, and metal salts, including $CdCl_2 \cdot 2H_2O$ and $NiCl_2 \cdot 2H_2O$ were purchased from Daejung Chemicals & Metals Co., Ltd. (Siheung, South Korea).

Synthesis of Schiff Base Derivatives

Pyridine-2-carboxaldehyde (100.58 mg, 0.94 mmol) or benzaldehyde (99.64 mg, 0.94 mmol) was added separately to a 50 mL ethanolic solution of the aromatic diamine (100 mg, 0.47 mmol). Acetic acid was added dropwise (4-5 drops) as a catalyst. The reaction mixture was stirred at room temperature for 1 h, followed by heating in a water bath at 60 °C and subsequent cooling to 4 °C. The resulting precipitates of SB-1 and SB-2 were collected by filtration, washed with ethanol, and dried under vacuum.

Sample Preparation for Sorption Studies

Metal cation solutions were prepared in the laboratory using salts $CdCl_2.2H_2O$, $NiCl_2.2H_2O$, and deionized water.

Ions Removal Measurements

The metal ions (Cd, Ni) removal potential of SB-1 and SB-2 was studied at different pH, using different dosages of Schiff base (SB-1 and SB-2), different contact times, and at different temperatures.

Optimal pH Studies

25 mL of 100 mgL^{-1} Cd^{+2} and Ni^{+2} solutions were mixed with 0.1 g of SB-1 and

SB-2 in a series of flasks, and these solutions were adjusted with varied pH values (2-12) using appropriate buffers. Solutions were shaken on a mechanical shaker for one hour. The concentrations of each metal were estimated before and after a one-hour agitation. The graph validated the ideal pH for optimal binding of SB-1 and SB-2 to metal ions.

Uptake Time Measurement

The uptake time of SB-1 and SB-2 was determined via batch mode at optimum pH, 0.1 g of both derivatives was taken in a series of conical Stoppard flasks, and then 25 mL ion solution was added. Solutions were agitated at room temperature at different time intervals (30 min, 1 h, 2 h, 6 h, 12 h, and 24 h). After the agitation, all the solutions were filtered off.

Uptake Capacity Measurement

The uptake capacity measurement of both derivatives was conducted in a batch manner. 25 mL of a 100 mgL^{-1} metal ions solution was taken in a series of stoppered flasks, and different dosages of both derivatives (100 mg, 150 mg, 200 mg, 250 mg, 300 mg, 350 mg, and 500 mg) was added to the flasks. The solution mixture was stirred at room temperature for one hour, and after agitation, the solutions were filtered off.

Temperature Measurement

SB-1 and SB-2 uptake potential was determined by shaking 25 mL of 100 mgL^{-1} metal ion solutions with 0.1 g of the derivatives in a sequence of conical flasks at varying temperatures (25, 35, 45, 55, 65, and 75 °C, respectively). Following agitation, the mixture was filtered out, and the optimum temperature for the metal ions adsorption was found.

The removal efficiency of SB-1 and SB-2 was determined by using equation 1.

$$\% \, Removal = \frac{(Co - Ce)}{Ce} \times 100 \qquad (1)$$

where C_o is the initial concentration while C_e is the equilibrium concentration of the metal ion.

The amounts of metal ions at equilibrium were determined by equation 2.

$$qe = \frac{(C_o - C_e)V}{W} \qquad (2)$$

Sorption Isotherm

In order to determine the removal of a particular quantity of a metal ion from a solution, the determination of the sorption capacity of an adsorbent is essential. Sorption capacity is typically determined using Freundlich and Langmuir sorption isotherm models. The linear Langmuir sorption equation is given in Equation (3).

$$\frac{Ce}{qe} = \left(\frac{1}{K_L Q_{max}}\right) + \left(\frac{C_e}{Q_{max}}\right) \qquad (3)$$

where Qe is amount of sorption per unit mass of the polymer at equilibrium (mg/g), Ce is equilibrium concentration (mg/L), qmaxis maximum theoretical saturation sorption capacity, and K_L is the energy of sorption.

Whereas, the equation (4) describes the linear regression of the Freundlich isotherm equation.

$$\ln qe = \ln k_f + \left(\frac{1}{n}\right) \ln C_e \qquad (4)$$

where K_F and n are Freundlich constants, qe is the quantity of metal adsorbed per unit mass of the adsorbent and Ce is the equilibrium metal ions concentration.

The total sorption capacities of SB-1 and SB-2 were determined by shacking 25 mL of Cd^{2+} and Ni^{2+} ion solutions with various concentration of adsorbents for 1 h at optimum pH and temperature in a mechanical shaker. The mixtures were filtered off, and the amount of metal ions in the filtrate was calculated by AAS.

Thermodynamic studies

The nature and mechanism of the adsorption process may be inferred from the thermodynamic characteristics such as Gibbs free energy (ΔG°), standard entropy change (ΔS°), and heat of sorption (ΔH°). The sorption process of heavy metal ions by adsorbents from aqueous solution is determined by observing their thermodynamic behavior. Equations for the determination of thermodynamic parameters are given below.

$$K_L = \frac{qe}{Ce} \quad (5)$$

$$\Delta G^0 = -RT \ln K_L \quad (6)$$

$$\ln K_L = -\frac{\Delta G^o}{RT} = -\left(\frac{\Delta H^o}{RT}\right) + \left(\frac{\Delta S^o}{R}\right) \quad (7)$$

where Ce is the adsorbate concentration at equilibrium (mg/L), qe is the sorption capacity at equilibrium (mg/g), and K_L is the sorption distribution coefficient, ΔG° is the Gibbs free energy change (J/mol), ΔS° is the standard change of entropy (J/mol/K^{-1}), ΔH° is the standard enthalpy change (J/mol), T is the temperature (K) and R is the universal gas constant (8.314 J/mol/K).

Kinetics Studies

Adsorption kinetic study is important for designing any adsorption system because it gives information about adsorbent performance and the rate of the adsorption process [12]. For kinetics studies, two commonly used models, the pseudo-first-order (PFO) model and pseudo-second-order (PSO) model, were investigated to predict the adsorption of Cd^{2+} and Ni^{2+} ions on SB-1 and SB-2 adsorbents. The pseudo-first-order and pseudo-second-order models' linearized regression is represented by equations (8) and (9), respectively.

$$\ln(qeqt) = \ln(qe) - k1t \quad (8)$$

$$\frac{t}{qt} = \frac{1}{k2qe^2} + \left(\frac{1}{qe}\right)t \quad (9)$$

Characterization of Schiff Base Derivatives (SB-1 and SB-2)

The formation and purity of the products were examined using TLC aluminum cards acquired from E. Merck, Germany. The FTIR absorption spectra were obtained in the range 4000-500 cm^{-1} using a Jasco-320-A spectrometer in DMSO, whereas the ^1H NMR spectra were measured in ppm (δ) using a Bruker-AV-400 spectrometer. A JEOL-600H-2 spectrometer was used for obtaining the FAB-MS spectra in negative mode in *m/z* ratio. The residual metal ion concentrations were estimated using an AA-7000 Atomic Absorption Spectrometer.

Results and Discussion

Synthesis and Characterization of Adsorbents

Schiff base derivatives (SB-1 and SB-2) were synthesized by a simple condensation process with 81.5 and 83.5 percent yield, as shown in the scheme (Fig. 1).

The structures of the synthesized Schiff base derivatives (SB-1 and SB-2) were

confirmed through spectroscopic analyses. FTIR spectra of both compounds exhibited characteristic absorption bands at 1623 cm^{-1} (SB-1) and 1630 cm^{-1} (SB-2) as depicted in Fig. 2(a) and 2(b), respectively, which correspond to the stretching vibrations of the imine (–C=N) group, confirming successful condensation and formation of the Schiff bases [5]. The UV–Vis spectra further supported the structures of SB-1 and SB-2. For SB-1, absorption maxima were observed at 246, 293, and 357 nm, while SB-2 displayed bands at 256, 288, and 365 nm, as shown in Fig. 2(c) and 2(d), respectively.

The higher-energy bands were attributed to π-π* transitions of the conjugated double bonds, whereas the lower-energy bands at 357 and 365 nm corresponded to n-π* transitions associated with the imine (–C=N) groups, providing additional evidence for Schiff base formation [5,13]. The ^{1}H-NMR spectra (recorded on AV-400 MHz in DMSO-d_6) showed distinct downfield singlet peaks at δ 8.57 (SB-1) and δ 8.58 (SB-2) as presented in Fig. 2(e) and 2(f), respectively, which were assigned to the azomethine protons (–CH=N). These characteristic signals confirmed the presence of the imine functionality. The obtained data are consistent with previously reported values for similar Schiff base derivatives [6,14,15]. Further confirmation was obtained from FAB-MS analysis. SB-1 exhibited a molecular ion peak at m/z 390.2, corresponding to the molecular formula $C_{26}H_{22}N_4$, while SB-2 showed a molecular ion peak at m/z 388.1, consistent with the formula $C_{28}H_{24}N_2$. These mass spectral data further validated the successful synthesis of both derivatives.

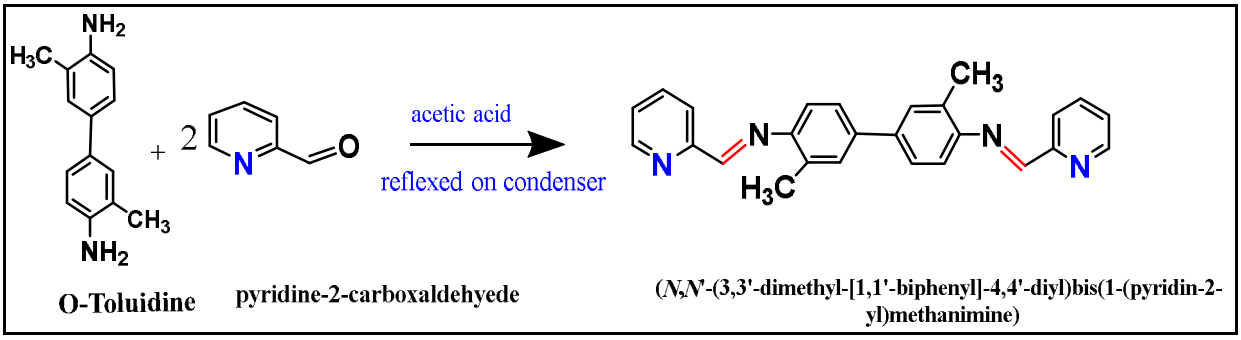

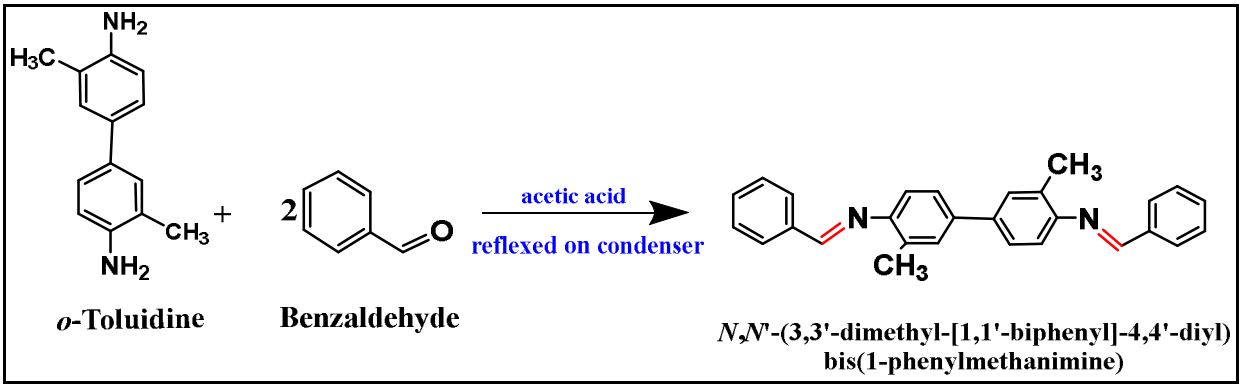

Figure 1. **Preparation of SB-1 and SB-2**

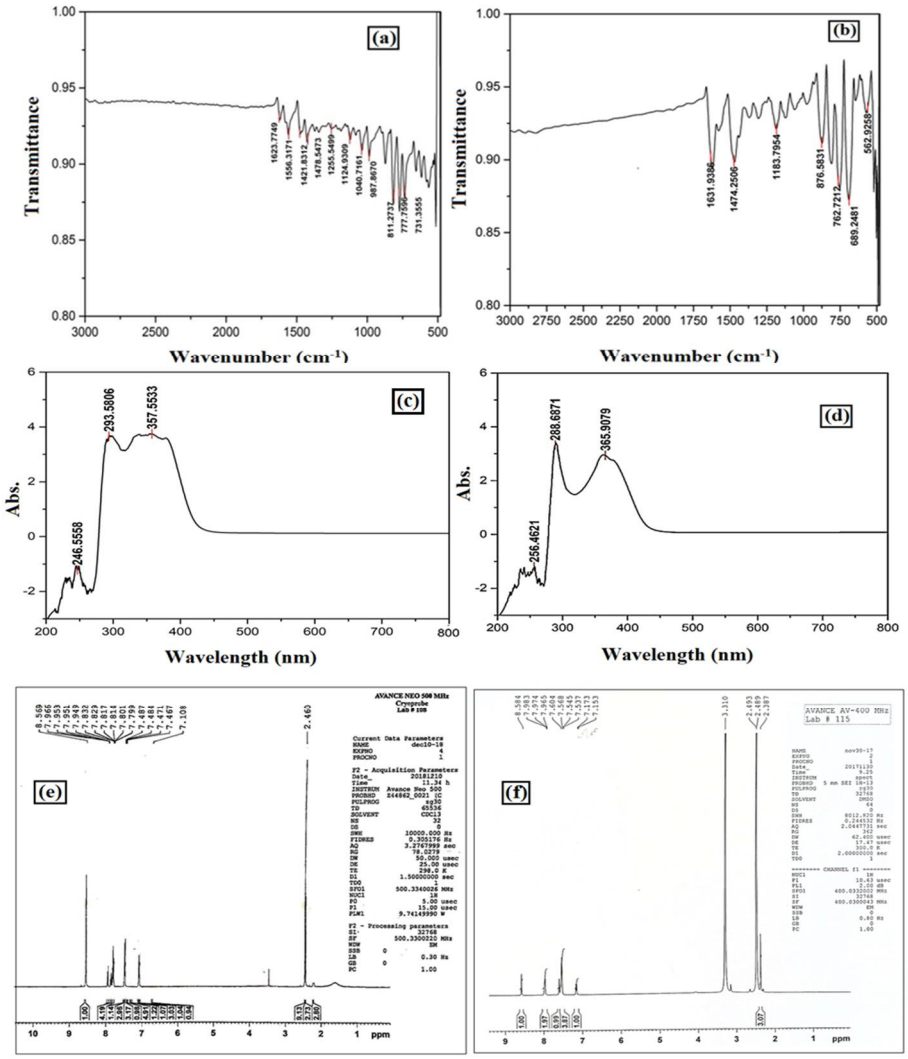

Figure 2. **FTIR spectra (a, b), UV–Vis spectra (c, d), and ^{1}H NMR spectra (e, f) of SB-1 and SB-2**

Metal Removal Studies

Effect of pH

The influence of pH on the adsorption of Cd(II) and Ni(II) ions by SB-1 and SB-2 was examined under batch conditions, and the results are shown in Fig. 3. For SB-1, the maximum uptake of Cd(II) and Ni(II) occurred at pH 8 and pH 6, respectively; whereas, SB-2 displayed the highest adsorption for both ions at pH 8. These results suggest that efficient adsorption takes place under mildly acidic to mildly basic conditions. At low pH, the adsorption capacity decreased significantly, likely due to protonation of the sorbent surface, which causes electrostatic repulsion between the positively charged adsorbent surface and the metal cations. Conversely, at highly basic pH values, a decline in adsorption was observed, which can be attributed to the precipitation of metal ions as insoluble hydroxides rather than adsorption onto the sorbents [5,16]. Based on these findings, pH 6 and 8 were selected as the optimum conditions for Cd(II) and Ni(II) adsorption by SB-1, and pH 8 was chosen as the optimum for SB-2. These observations are consistent with previously reported studies on heavy metal adsorption using Schiff base derivatives and related sorbents [17,18].

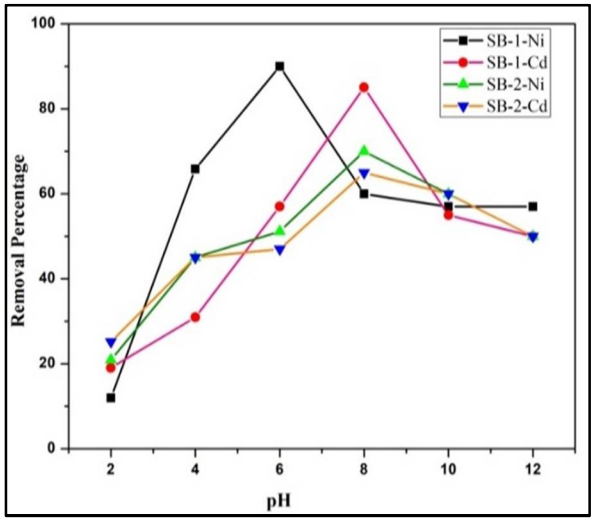

Figure 3. **Effect of pH on the process of adsorption**

Effect of Exposure Time

The influence of contact time on the adsorption of Cd(II) and Ni(II) ions was evaluated under batch conditions. As shown in Fig. 4, the adsorption rate was initially rapid within the first hour, followed by a gradual decline until equilibrium was reached. The high initial uptake can be attributed to the strong affinity of metal ions toward the active binding sites on the sorbent surface. With increasing time, the number of available sites decreased, leading to a slower adsorption rate as the system approached equilibrium [18].

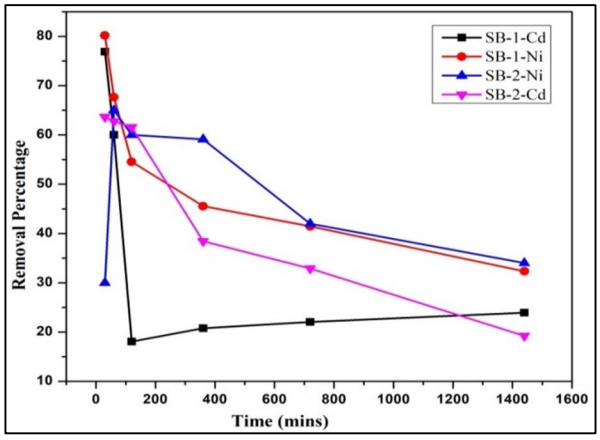

Figure 4. **Effect of exposure time on the process of adsorption**

Quantitatively, SB-1 achieved 80% removal of Ni(II) and 78% removal of Cd(II) within 30 min, whereas SB-2 exhibited a removal efficiency of 66% for Ni(II) at 60 min and 62% for Cd(II) at 30 min**.** These results indicate that SB-1 demonstrated comparatively faster and higher adsorption efficiency than SB-2. The observed trend is consistent with previous studies on Schiff base-derived sorbents for heavy metal removal [19].

Effect of Adsorbent Dosage

The effect of adsorbent dosage on the removal of Cd(II) and Ni(II) ions was investigated by varying the amount of SB-1 and SB-2 in the range of 0.1-0.5 g, using a fixed initial concentration of 100 mg/L for both metal ions (Fig. 5). The results demonstrated that metal ion uptake increased with increasing adsorbent dose, reaching a maximum at 0.5 g for both derivatives. This enhancement in removal efficiency can be attributed to the higher number of available active binding sites provided by the greater adsorbent mass, which facilitated enhanced metal-ligand interactions. These findings are consistent with earlier reports on Schiff base-based adsorbents [20]. Furthermore, a variation in the percentage removal of Cd(II) and Ni(II) ions was observed, which can be rationalized based on their ionic radii. Ni(II) (0.69 Å) exhibited higher adsorption efficiency compared to Cd(II) (0.96 Å). The smaller ionic size of Ni(II) enhances its diffusion rate in aqueous solution and enables stronger competition for active adsorption sites, resulting in a removal trend of Ni(II) > Cd(II). This behavior is in agreement with previously reported adsorption studies [18].

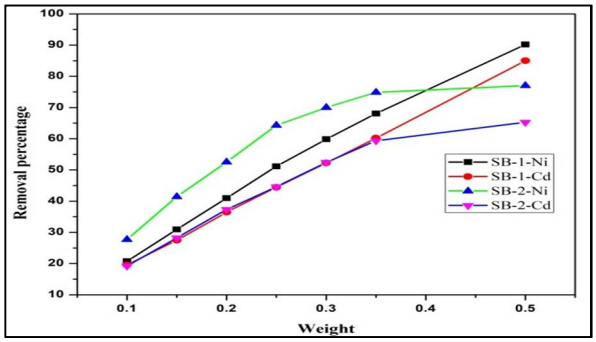

Figure 5. **Effect of adsorbent dosage on the adsorption process**

Effect of Temperature

The influence of temperature on the adsorption of Ni(II) and Cd(II) ions by SB-1 and SB-2 was examined in the range of 25-55 °C (Fig. 6).

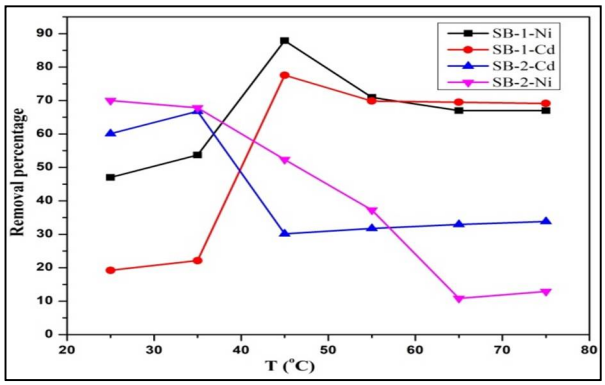

Figure 6. **Effect of temperature on the process of adsorption**

For SB-1, adsorption efficiency increased with rising temperature, indicating an endothermic adsorption process. The enhanced uptake at elevated temperatures can be attributed to stronger interactions between the active sites of the Schiff base ligands and the metal ions, as well as increased mobility of the ions in solution. Maximum adsorption for both Ni(II) and Cd(II) was observed at 45 °C, after which equilibrium was attained, and further uptake proceeded slowly. In contrast, SB-2 displayed a different adsorption behavior. At lower temperatures (25-35 °C), SB-2 exhibited comparatively higher removal efficiencies for both metal ions. However, as the temperature increased beyond this range, a gradual decline in adsorption capacity was observed, suggesting that the process is more favorable under mild thermal conditions. These contrasting thermodynamic profiles highlight the role of structural differences between SB-1 and SB-2 in governing their sorption behavior. Similar observations regarding the temperature dependence of Schiff base–metal ion adsorption have been reported in earlier studies [6].

Isotherm Studies

The relationship between the equilibrium concentration of metal ions in solution and the amount adsorbed by the sorbents was analyzed through equilibrium studies. The adsorption data were fitted to the Langmuir and Freundlich isotherm models to evaluate the adsorption characteristics (Fig. 7 a-d and Fig. 8 a-d).

Table 1a and 1b, among the two models, the Langmuir isotherm provided the best fit to the experimental results, indicating that adsorption occurred on a homogeneous surface with uniformly distributed active chelating sites. The maximum sorption capacity (Qmax) values obtained from the Langmuir model were 16.89 mg/g (Ni) and 8.05 mg/g (Cd) for SB-1, while for SB-2 they were 12.66 mg/g (Ni) and 7.42 mg/g (Cd). These results suggest that both adsorbents exhibited a higher affinity toward Ni(II) ions compared to Cd(II). The strong agreement between the model and the experimental data was confirmed by the high coefficients of determination (R^2) for the Langmuir model, which were 0.999 (Ni) and 0.9909 (Cd) for SB-1, and 0.998 (Ni) and 0.9945 (Cd) for SB-2. Furthermore, the dimensionless separation factor (R_L), which ranged between 0.001-0.003, confirmed that the adsorption of both Ni(II) and Cd(II) ions was highly favorable under the tested conditions.

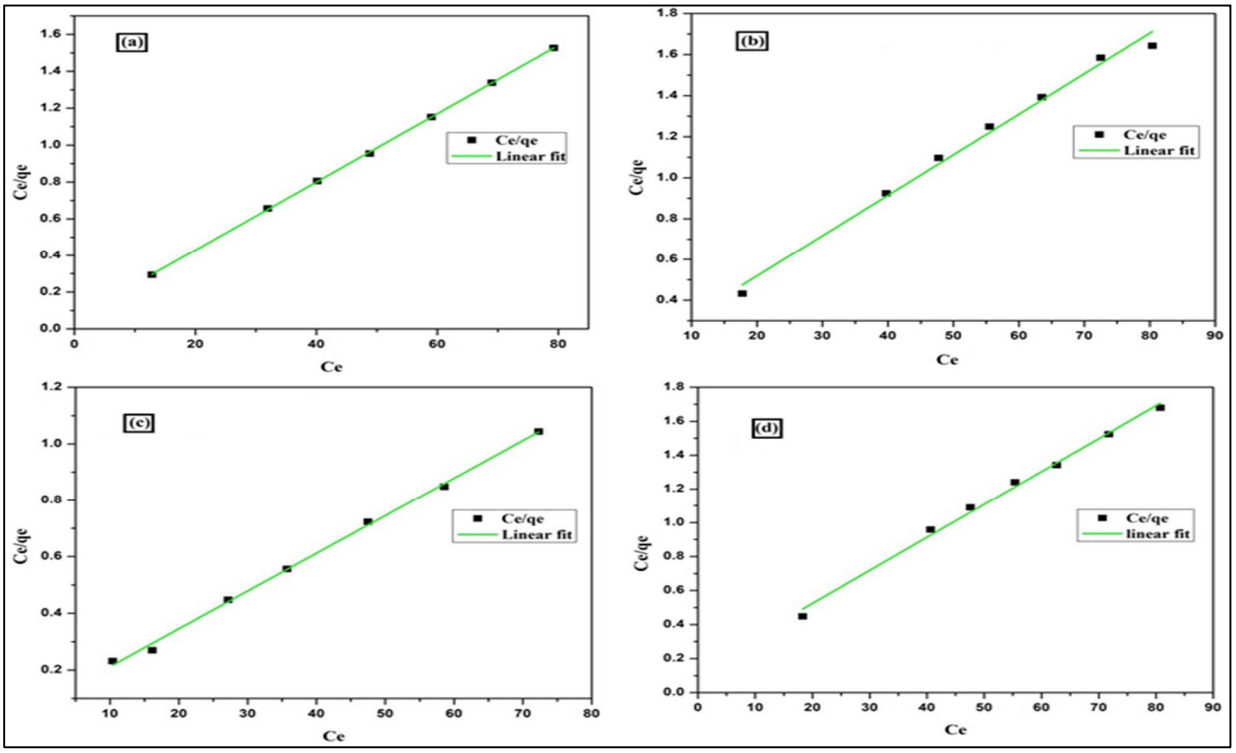

Figure 7. **Langmuir isotherm plots for the adsorption of Ni(II) and Cd(II) ions by SB-1 (a, b) and SB-2 (c, d)**

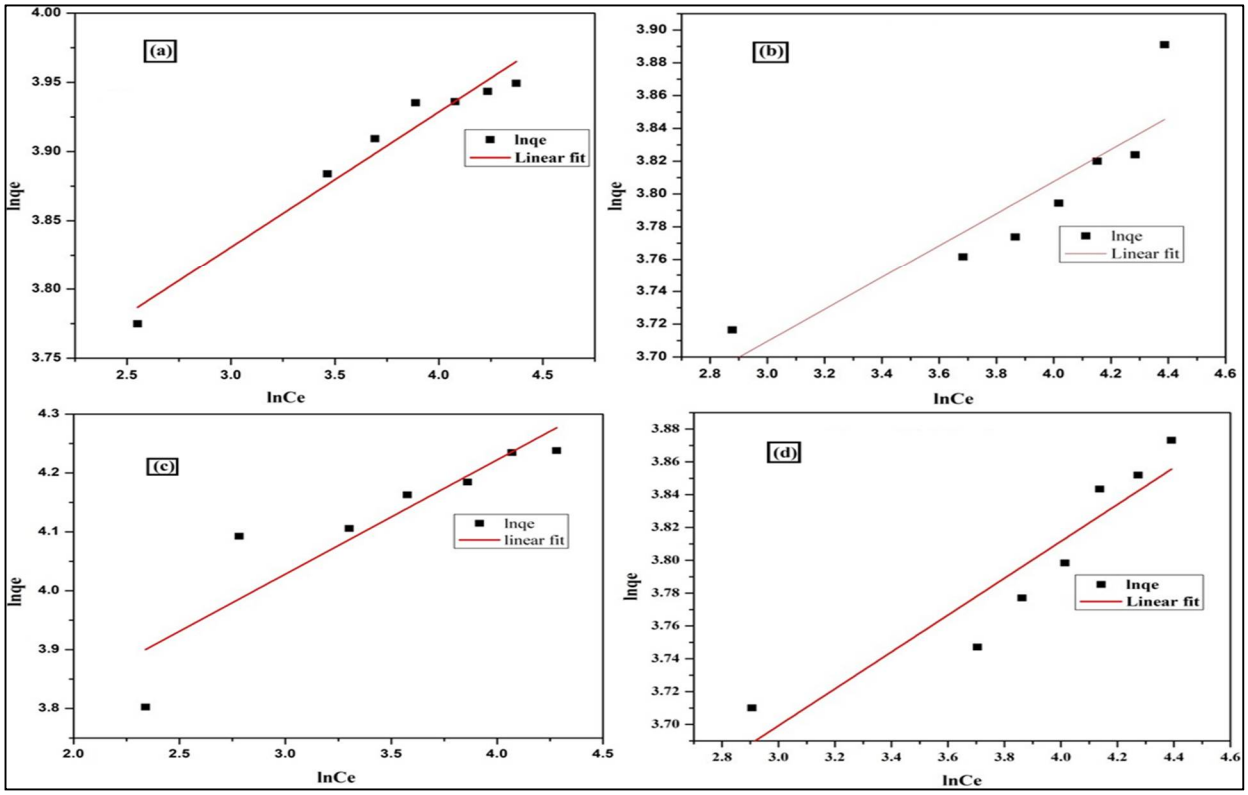

Figure 8. **Freundlich isotherm plots for the adsorption of Ni(II) and Cd(II) ions by SB-1 (a, b) and SB-2 (c, d)**

Table (1a). **Langmuir isotherm model parameters obtained from adsorption studies.**

	Langmuir Isotherm Model			
	Q_{max} (mg/g)	K_L (L mg^{-1})	R_L	R^2
SB-1-Ni	16.8919	3.2000	0.0031	0.9990
SB-1-Cd	8.0451	6.2778	0.0016	0.9909
SB-2-Ni	12.658	5.9398	0.0017	0.9980
SB-2-Cd	7.4184	6.9128	0.0014	0.9945

Table (1b). **Freundlich isotherm model parameters obtained from adsorption studies.**

	Freundlich Isotherm Model			
	Q_{max}(mg/g)	1/n	K_f (L g^{-1})	R^2
SB-1-Ni	0.2827	0.0979	0.1683	0.9586
SB-1-Cd	0.2928	0.0980	0.1742	0.8132
SB-2-Ni	0.2902	0.1941	0.1038	0.79183
SB-2-Cd	0.2974	0.1123	0.1640	0.84872

Kinetics Studies

For sorption of Ni and Cd ions, the pseudo-first-order and pseudo-second-order models were investigated. All the experimental parameters and plots are given in Table 2a and 2b, and presented in Fig. 9.

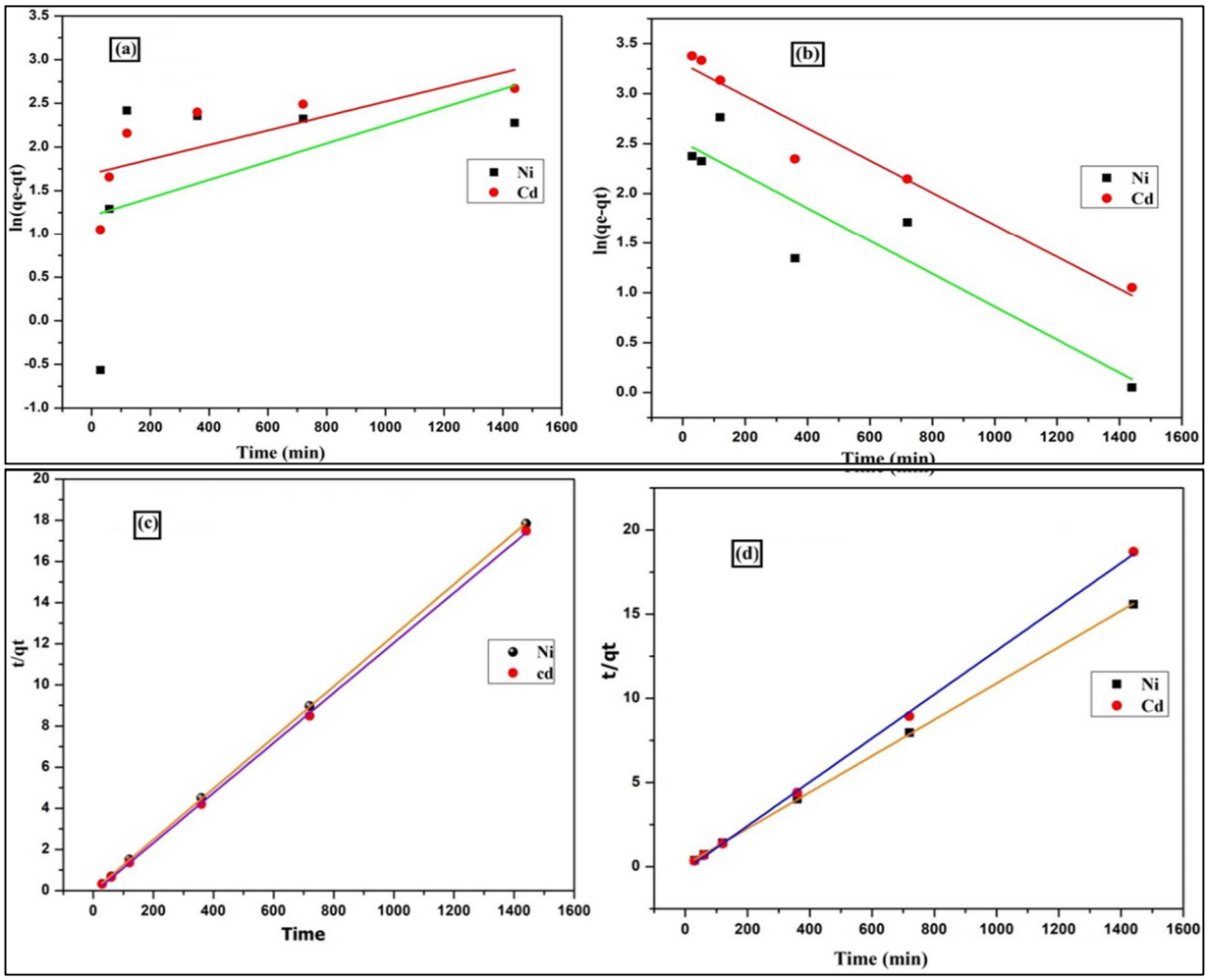

Figure 9. **Pseudo-first-order and pseudo-second-order kinetic model plots for the adsorption of Ni(II) and Cd(II) ions by SB-1 (a, c) and SB-2 (b, d)**

Results showed that all the experimental data were well fitted to the pseudo-second-order model, and the values of the correlation coefficient were closely related to 1. Moreover, the sorption capacity obtained from the pseudo-second-order plot is close to experimental values. As a result, the pseudo second order kinetic model is considered to be more suitable to describe the kinetics of the metal ion adsorption processes than the pseudo first order kinetic model. This fitness indicated that the adsorption of these metal ions involves a chemisorption process, where the sorption phase involves the valence force through complexation, coordination, or chelation. This finding is consistent with other reported works [21-23].

Table (2a). **Pseudo-first-order kinetic model parameters for sorption studies.**

	Pseudo-First-Order-Model			
	qe(exp) (mg/g)	qe(cal) (mg/g)	k_1 (min^{-1})	R^2
SB-1-Ni	80.189	3.356	3.333	0.03
SB-1-Cd	80.102	5.444	2.666	0.550
SB-2-Ni	91.736	12.359	-1	0.957
SB-2-Cd	77.512	9.2636	0.0002	0.8179

Table (2b). **Pseudo-second-order kinetic model parameters for sorption studies.**

	Pseudo-Second-Order-Model			
	qe(exp) (mg/g)	qe(cal) (mg/g)	K_2 (min^{-1})	R^2
SB-1-Ni	80.189	80.645	0.028	1
SB-1-Cd	80.102	81.967	0.001	1
SB-2-Ni	91.736	92.592	0.0011	0.999
SB-2-Cd	77.512	76.923	0.0011	0.999

Thermodynamic Studies

Thermodynamic studies were used to determine the spontaneity of the sorption process. Values of ΔG°, ΔH°, and ΔS° are given in Table 3 for both adsorbents. In the case of the test sorbent SB-1, the Gibbs free energy parameter was obtained in negative values that suggested the spontaneity of adsorption reactions. Gibbs free energy values become more negative when the temperature rises, indicating high sorption capacity at high temperature. The positive values of ΔS° and ΔH° revealed that the sorption process occurred with increased randomness, was irreversible, and endothermic. Similar results were obtained by Arshadi et al [24]. In the case of SB-2, the Gibbs free energy parameter ΔG° was also obtained in negative values, which suggested the spontaneity of adsorption reactions. With an increase in temperature, the values of ΔG° became more positive, indicating low sorption capacity at high temperature [20]. The negative values of ΔS° and ΔH° revealed that the sorption process was reversible and exothermic.

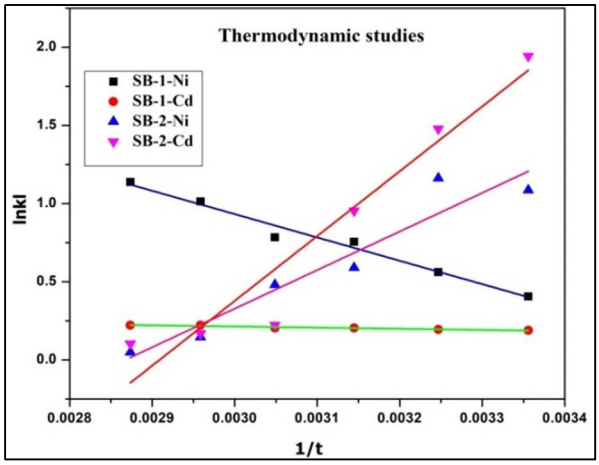

Figure 9. **Graphical representation of thermodynamic studies for the adsorption of Ni(II) and Cd(II) ions by SB-1 and SB-2**

Table 3. **Thermodynamic parameters for adsorption of Ni(II) and Cd(II) ions by SB-1 and SB-2.**

	T (k)	ΔG° J mol-1	ΔH° kJ mol-1	ΔS° kJ/mol
SB-1-Ni	298	-1005	12.415	44.99
	308	-1437		
SB-1-Cd	298	-411	1.0895497	5.0274758
	308	-433		
SB-2-Ni	298	-2689	-20.518952	-58.8498176
	308	-2976		
SB-2-Cd	298	-4811	-34.46153	-10026.684
	308	-3783		

Conclusion

The adsorption behavior of Ni(II) and Cd(II) ions onto the synthesized imine-based sorbents was systematically evaluated through equilibrium isotherm studies. The experimental data were well described by the Langmuir model rather than the Freundlich model, indicating monolayer adsorption on homogeneous surfaces with uniformly distributed chelating sites. Based on the Langmuir model, SB-1 exhibited higher maximum adsorption capacities (Qmax) for both Ni(II) (16.89 mg/g) and Cd(II) (8.05 mg/g) compared to SB-2, which showed Qmax values of 12.66 mg/g for Ni(II) and 7.42 mg/g for Cd(II). This trend demonstrates the superior adsorption efficiency of SB-1, likely due to the presence of pyridine nitrogen atoms that enhance metal-ligand interactions. The strong agreement between the Langmuir model and the experimental data was further supported by high coefficients of determination (R^2), confirming the reliability of the fitting. Moreover, the dimensionless separation factor (R_L) values, lying between 0.001 and 0.003, indicated highly favorable adsorption under the studied conditions. Kinetic investigations revealed that the adsorption process followed a pseudo-second-order model, suggesting a chemisorption mechanism. Thermodynamic parameters demonstrated that adsorption onto SB-1 was spontaneous, irreversible, and endothermic, whereas SB-2 exhibited spontaneous, reversible, and exothermic behavior. Overall, the results highlight the potential of these imine derivatives, particularly SB-1, as effective sorbents for the removal of toxic Ni(II) and Cd(II) ions from aqueous environments.

Conflict of Interest

The authors declare that they have no known competing financial interests or personal relationships that could have appeared to influence the work reported in this paper.

References

1. M. Albratty and H. A. Alhazmi, *Arab. J. Chem*., 15 (2022) 103846. doi:10.1016/j.arabjc.2022.103846.
2. Md. B. Islam, Md. I. Islam, N. Nath, T. B. Emran, Md. R. Rahman, R. Sharma and M. M. Matin, *Biomed. Res. Int*., 2023 (2023) 9967591. doi: 10.1155/2023/9967591.
3. K. K. Joshi, Chemistry with Schiff Bases of Pyridine Derivatives: Their Potential as Bioactive Ligands and Chemosensors, In: Exploring Chemistry with Pyridine Derivatives (S. Pal, Ed.), IntechOpen, London (2022). doi:10.5772/intechopen.106749.
4. S. Pal, Pyridine: A Useful Ligand in Transition Metal Complexes, In: Pyridine (P. P. Pandey, Ed.), IntechOpen, (2018). doi: 10.5772/intechopen.76986.
5. N. Jamil, N. Khan, R. Jabeen, R. Mehmood and N. Naheed, *Int. J. Environ. Anal. Chem*., 101 (2021) 2510. doi: 10.1080/03067319.2019.1694669.
6. N. Khan, N. Jamil, R. Jabeen, M. M. Akhtar, H. Ali, R. Mehmood, R. Orfali, S. Perveen, J. Peng and A. M. Al-Taweel, *Front. Environ. Sci*., 11 (2023) 1128256. doi: 10.3389/fenvs.2023.1128256.
7. Q. Fu, T. Zhang, X. Sun, S. Zhang, G. I. N. Waterhouse, C. Sun, H. Li and S. Ai, *Chem. Eng. J*., 454 (2023) 140154. doi: 10.1016/j.cej.2022.140154.
8. A. Singh and A. Kaushik, *J. Clean. Prod*., 315 (2021) 127940. doi: 10.1016/j.jclepro.2021.127940.
9. G. Genchi, A. Carocci, G. Lauria, M. S. Sinicropi and A. Catalano, *Int. J.*

Environ. Res. Public Health, 17 (2020) 679.
doi: 10.3390/ijerph17030679.

10. A. Khan, S. Khan, M. A. Khan, Z. Qamar and M. Waqas, *Environ. Sci. Pollut. Res*., 22 (2015) 13772. doi: 10.1007/s11356-015-4881-0.
11. S. Mitra, A. J. Chakraborty, A. M. Tareq, T. B. Emran, F. Nainu, A. Khusro, A. M. Idris, M. U. Khandaker, H. Osman, F. A. Alhumaydhi and J. Simal-Gandara, *J. King Saud Univ. Sci.,* 34 (2022) 101865. doi: 10.1016/j.jksus.2022.101865.
12. J. Wang and X. Guo, *J. Hazard. Mater*., 390 (2020) 122156. doi: 10.1016/j.jhazmat.2019.122156.
13. A. N. Alhakimi, *Egypt. J. Chem*., 63 (2020) 1509. doi: 10.21608/ejchem.2020.20906.2256.
14. D. Ozkir, *J. Electrochem. Sci. Technol*., 10 (2019) 37. doi: 10.5229/JECST.2019.10.1.37.
15. M. A. El-Ghamry, F. M. Elzawawi, A. A. A. Aziz, K. M. Nassir and S. M. Abu-El-Wafa, *Sci. Rep*., 12 (2022) 17942. doi: 10.1038/s41598-022-22713-z.
16. X. Zeng, G. Zhang and Z. Wu, *Environ. Sci. Pollut. Res*., 29 (2022) 30324. doi: 10.1007/s11356-021-17949-7.
17. R. Hassan, H. Arida, M. Montasser and N. Abdel Latif, *J. Chem*., 1 (2013) 240568. doi: 10.1155/2013/240568.
18. T. C. Egbosiuba, A.S. Abdulkareem, A.S. Kovo, E.A. Afolabi, J.O. Tijani, M.T. Bankole, S. Bo, W. D. Roos, *Sci. Rep*., 11 (2021) 75. doi:10.1038/s41598-020-79857-z.
19. Z. Sheikh, M. Amin, N. Khan, M. N. Khan, S. K. Sami, S. B. Khan and C. K. Cheng, *Chemosphere*, 279 (2021) 130545. doi:10.1016/j.chemosphere.2021.130545
20. A. A. Younes and H. H. El-Maghrabi, *Sep. Sci. Technol*., 55 (2020) 1589. doi: 10.1080/01496395.2019.1604758.
21. M. A. Betiha, Y. M. Moustafa, M. F. El-Shahat and E. Rafik, *J. Hazard. Mater*., 397 (2020) 122675. doi: 10.1016/j.jhazmat.2020.122675.
22. A. Dadrasnia, K. S. C. Wei, N. Shahsavari, M. S. Azirun and S. Ismail, *Int. J. Environ. Res. Public Health*, 12 (2015) 15321. doi: 10.3390/ijerph121214985.
23. M. K. Moftakhar, M. R. Yaftian and M. Ghorbanloo, *Int. J. Environ. Sci. Technol*., 13 (2016) 1707. doi: 10.1007/s13762-016-0969-4.
24. M. Arshadi, M. J. Amiri and S. Mousavi, *Water. Res. Ind*., 6 (2014) 1. doi: 10.1016/j.wri.2014.06.001.